Periodic solutions in next generation neural field models

Carlo R. Laing[1,*] and Oleh E. Omel'chenko[2,†]

[1]School of Mathematical and Computational Sciences,
Massey University, Private Bag 102-904 NSMC, Auckland, New Zealand
[2]Institute of Physics and Astronomy, University of Potsdam,
Karl-Liebknecht-Str. 24/25, 14476 Potsdam, Germany.

(Dated: June 21, 2023)

We consider a next generation neural field model which describes the dynamics of a network of theta neurons on a ring. For some parameters the network supports stable time-periodic solutions. Using the fact that the dynamics at each spatial location are described by a complex-valued Riccati equation we derive a self-consistency equation that such periodic solutions must satisfy. We determine the stability of these solutions, and present numerical results to illustrate the usefulness of this technique. The generality of this approach is demonstrated through its application to several other systems involving delays, two-population architecture and networks of Winfree oscillators.

INTRODUCTION

The collective behaviour of large networks of neurons is a topic of ongoing interest. One of the simplest forms of behaviour is a periodic oscillation, which manifests it-

N synaptically coupled theta neurons described by

$$\frac{d_{\ j}}{dt} = 1 \quad \cos_{\ j} + (1 + \cos_{\ j})(_{\ j} + I_{\ j}); \quad j = 1; : : : ; N; \tag{1}$$

where each $_{j}$

II. PERIODIC STATES

In this paper we focus on states with periodically os-

of the choice of the real-valued periodic function $W(x;t)$, parameters $2 C_{up} = \{z 2 C : \mathrm{Im}\, z > 0\}$ and $! > 0$, for every xed $x 2 [0;2\ ]$ Eq. (7) has a unique stable 2-periodic solution $U(x;t)$ that lies entirely in the open unit disc D. Denoting the corresponding solution operator by

$$U : C_{per}([0;2\ ];R) \quad C_{up} \quad (0;1\ ) ! \quad C_{per}([0;2\ ];D);$$

we can write the 2-periodic solution of interest as

$$U(x;t) = U \quad W(x;t); \frac{_0 + i}{2!}; ! \quad : \qquad (10)$$

Note that $C_{per}([0;2\ ];R)$ here denotes the space of all real-valued continuous 2-periodic functions, while the notation $C_{per}([0;2\ ];D)$ stands for the space of all complex continuous 2-periodic functions with values in the open unit disc D. Importantly, the variable x appears in formula (10) as a parameter so that the function $W(x;\ ) 2 C_{per}([0;2\ ];R)$ with a xed x is considered as the rst argument of the operator U.

As for the operator U, although it is not expl.7or

equation (7). The linearization of Eq. (7) around this solution reads

$$\frac{dv}{dt} = M(x;t)v;$$

where

$$M(x;t) = 2i \quad W(x;t) + \quad + \frac{1}{2!}$$
$$+ 2i \quad W(x;t) + \quad \frac{1}{2!} \quad U(x;t):$$

Moreover, using (8) and (9), we can show that the above expression determines a function identical to the function $M(x;t)$ in (12). Recalling that $U(x;t)$ is not only a stable but also an asymptotically stable solution of Eq. (7), see Remark 1 in Appendix, we conclude that the corresponding Floquet multiplier lies in the open unit disc D. This ends the proof. ■

C. Numerical implementation

Eq. (11) describes a periodic orbit, and since Eq. (7) is autonomous we need to append a pinning condition in order to select a speci c solution of Eq. (11). For a solution of the type shown in Fig. 1 we choose

$$\int_0^{2\pi} dx \int_0^{2\pi} W(x;t)\sin(2t)dt = 0: \qquad (13)$$

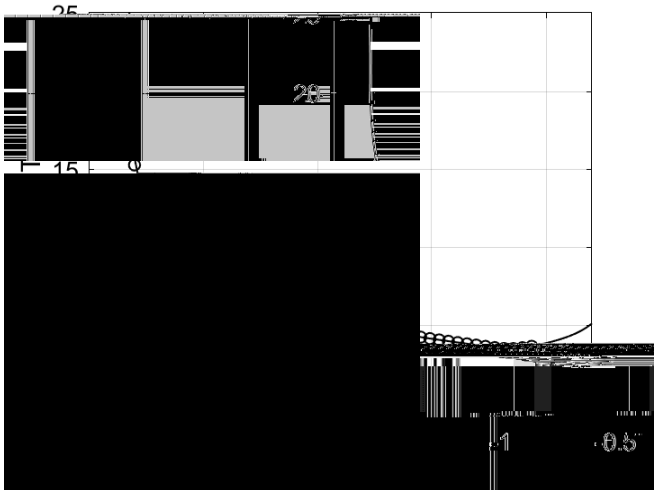

FIG. 2. Period of the type of solution shown in Fig. 1 as a function of ν_0 (solid curve). The circles show values measured from direct simulations of Eq. (4). Other parameters: $A = 5$, $\gamma = 1$, $\varepsilon = 0.01$.

Fig. 3. Such a solution does not have the spatio-temporal symmetry of the solution shown in Fig. 1. However, we can follow it in just the same way as the parameter ν_0 is varied, and we obtain the results shown in Fig. 4. This periodic orbit appears to be destroyed in a supercritical Hopf bifurcation as ν_0 is decreased through approximately 3.2, and become unstable to a wandering pattern at ν_0 is increased through approximately 2.34.

Note that the left asymptote in Fig. 2 coincides with the right asymptote in Fig. 4. On the other hand, we note that two patterns shown in Figs. 1 and 3 have different spatiotemporal symmetries, therefore due to topological reasons they cannot continuously transform into each other. Similar bifurcation diagrams where parameter ranges of two patterns with different symmetries are separated by heteroclinic or homoclinic bifurcations were found for non-locally coupled Kuramoto-type phase oscillators [42] and seem to be a general mechanism which, however, needs additional investigation.

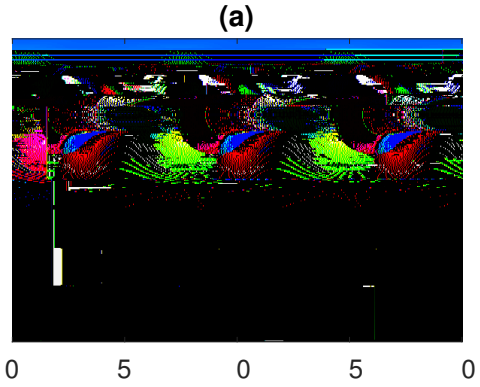

FIG. 3. Another periodic solution of Eq. (4). (a): $\arg(z(x;t))$. (b): $|z(x;t)|$. Parameters: $A = 5$, $\nu_0 = 2.5$, $\gamma = 1$, $\varepsilon = 0.01$.

FIG. 4. Period of the type of solution shown in Fig. 3 as a function of ν_0 (solid curve). The circles show values measured from direct simulations of Eq. (4). Other parameters: $A = 5$, $\gamma = 1$, $\varepsilon = 0.01$.

E. Stability of breathing bumps

Given a T-periodic solution $a(x;t)$ of Eq. (4), we can perform its linear stability analysis, using the approach proposed in [39]. Before doing this, we write

$$H_n(z) = a_n C_0 + 2\mathrm{Re}[D_n(z)]$$

where

$$D_n(z) = a_n \sum_{q=1}^{n} C_q z^q;$$

to emphasise that $H_n(z)$ is always real. Now, we insert the ansatz $z(x;t) = a(x;t) + v(x;t)$ into Eq. (4) and linearize the resulting equation with respect to small perturbations $v(x;t)$. Thus, we obtain a linear integro-

di erential equation

$$\frac{@v}{@t} = \quad (x;t)v + \quad \frac{i(1 + a(x;t))^2}{2} K \quad D_n^0(a)v + \overline{D_n^0(a)}\bar{v} \quad ; \tag{17}$$

where

$$(x;t) = [\, i(\ _0 + \quad K H_n(a)) \quad\quad](1 + a(x;t)) + i(1 \quad a(x;t)) \tag{18}$$

and

$$D_n^0(z) = \frac{d}{dz} D_n(z) = a_n \sum_{q=1}^{n} q C_q z^{q\ 1}:$$

Note that Eq. (17) coincides with the Eq. (5.1) from [40], except that the coe cients $a(x;t)$ and $(x;t)$ are now time-dependent. Since Eq. (17) contains the complex-conjugated term $\bar{v}$, it is convenient to consider this equation along with its complex-conjugate

$$\frac{@\bar{v}}{@t} = \ \bar{}(x;t)\bar{v} \quad\quad \frac{i(1 + \bar{a}(x;t))^2}{2} K \quad D_n^0(a)v + \overline{D_n^0(a)}\bar{v} \quad :$$

This pair of equations can be written in the operator form

$$\frac{dV}{dt} = A(t)V + B(t)V; \tag{19}$$

where $V(t) = (\, v_1(t); v_2(t))^T$ is a function with values in $C_{per}([0;2\ ];C^2)$, and

$$A(t)V = \begin{pmatrix} (x;t) & 0 \\ 0 & \ \bar{}(x;t) \end{pmatrix} \begin{pmatrix} v_1 \\ v_2 \end{pmatrix};$$

and

$$B(t)V = \frac{i}{2} \begin{pmatrix} (1 + a(x;t))^2 & 0 \\ 0 & (1 + \bar{a}(x;t))^2 \end{pmatrix} \begin{pmatrix} 0 & K (D_n^0(a)v_1) \\ @ K \overline{D_n^0(a)}v_2 & 1 A \end{pmatrix} : \tag{20}$$

For every xed t the operators $A(t)$ and $B(t)$ are linear operators from $C_{per}([0;2\ ];C^2)$ into itself. Moreover, they both depend continuously on t and thus their norms are uniformly bounded for all $t \ 2\ [0;T]$.

Recall that the question of linear stability of $a(x;t)$ in Eq. (4) is equivalent to the question of linear stability of the zero solution in Eq. (17), and hence to the question of linear stability of the zero solution in Eq. (19). Moreover, using the general theory of periodic di erential equations in Banach spaces, see [13, Chapter V], the last question can be reduced to the analysis of the spectrum of the monodromy operator $E(T)$ de ned by the operator exponent

$$E(t) = \exp \int_0^t (A(t') + B(t'))dt' \ :$$

The analysis of Eq. (19) in the case when $A(t)$ is a matrix multiplication operator and $B(t)$ is an integral operator similar to (20) has been performed in [39, Section 4]. Repeating the same arguments we can demonstrate that the spectrum of the monodromy operator $E(T)$ is bounded and symmetric with respect to the real axis of the complex plane. Moreover, it consists of two qualitatively different parts:

(i) the essential spectrum, which is given by the formula

$$_{ess} = \left(\exp \int_0^T (x;t)dt \ : x \ 2\ [0;2\ ] \right) [\, f\ c.c.g \tag{21}$$

(ii) the discrete spectrum $_{disc}$ that consists of nitely many isolated eigenvalues , which can be found using a characteristic integral equation, as explained in [39, Section 4].

Note that if $a(x;t)$ is obtained by solving the self-consistency equation (11) and hence it satis es

$$a(x;t=!) = U(x;t) = U \quad W(x;t); \frac{_0 + i}{2!}; ! \quad ;$$

where $(W(x;t);!)$ is a solution of Eq. (11), then we can use Proposition 1 and formula (18) to show

$$\exp \int_0^T (x;t)dt \quad < 1 \quad \text{for all} \quad x \ 2\ [0;2\ ]:$$

In this case, the essential spectrum $_{ess}$ lies in the open unit disc D and therefore it cannot contribute to any linear instability of the zero solution of Eq. (19).

To illustrate the usefulness of formula (21), in Fig. 5 (a) we plot the essential spectrum for the periodic solution shown in Fig. 1. In Fig. 5 (b) we show the Floquet multipliers of the same periodic solution, where we have found the solution and its stability in the conventional way, of discretizing the domain and nding a periodic solution of a large set of coupled ordinary di erential equations. In panel (b) we see several real Floquet multipliers that do not appear in panel (a); these are presumably part of the discrete spectrum. Note that calculating the discrete spectrum by the method of [39, Section 4] is numerically di cult, so we do not do that here.

F. Formula for ring rates

One quantity of interest in a network of model neurons such as (1) is their ring rate. The ring rate of the kth neuron is de ned by

$$f_k = \frac{1}{2} \quad \frac{d_k}{dt} D(94.04g\ 9d\ brsoperators$$

FIG. 5. (a) The essential spectrum given by (21) for the periodic solution shown in Fig. 1. (b) Floquet multipliers of the same periodic solution found using the technique explained at the start of Sec. II. For both calculations the spatial domain has been discretized using 512 evenly spaced points.

average ring rate

$$f(x) = \frac{1}{\#\{k : |x_k - x| <= \sqrt{N}\}} \sum_{|x_k - x| <= \sqrt{N}} f_k; \quad (22)$$

where $x_k = 2\pi k/N$ is the spatial positions of the kth neuron and the averaging takes place over all neurons in the $(= \sqrt{N})$-vicinity of the point $x \in [0; 2\pi]$. Note that while the individual ring rates f_k are usually randomly distributed due to the randomness of the excitability parameters $_k$, the average ring rate $f(x)$ converges to a continuous (and even smooth) function for $N \to \infty$. Moreover, the exact prediction of the limit function $f(x)$ can be given, using only the corresponding solution $z(x; t)$ of Eq. (4). To show this, we write Eq. (1) as

$$\frac{d}{d} \frac{d}{d} \frac{d}{d} \frac{d_k}{}$$

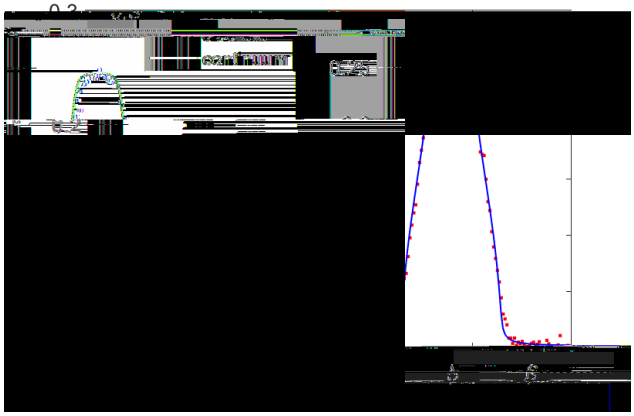

FIG. 6. Average ring rate for a pattern like that shown in Fig. 1. The curve shows f (x) as given by (26). The dots

$$\frac{@u}{@t} = \frac{(i_{u} \quad)(1+u)^2 \quad i(1 \quad u)^2}{2} + \frac{i(1+u)^2}{2}[w_{ee}KH_n(u) \quad w_{ei}KH_n(v)]; \quad (31)$$

$$\frac{@v}{@t} = \frac{(i_{v} \quad)(1+v)^2 \quad i(1 \quad v)^2}{2} + \frac{i(1+v)^2}{2}[w_{ie}KH_n(u) \quad w_{ii}KH_n(v)] \quad (32)$$

where $u(x;t)$ is the complex-valued order parameter for the excitatory population and $v(x;t)$ is that for the inhibitory population. The non-negative connectivity kernel between and within populations is the same:

$$K(x) = \frac{1}{2}(1+\cos x)$$

perio2(eork)-2ualliedwaves

FIG. 9. Period, T, of a modulated travelling wave solution of Eqs. (31){(32) as a function of heterogeneity strength . Circles are from direct simulation of Eqs. (31){(32). Other parameters are as in Fig. 8.

The results of varying the heterogeneity strength are shown in Fig. 9. Increasing heterogeneity decreases the period of oscillation, and eventually the travelling wave appears to be destroyed in a saddle-node bifurcation.

We conclude this section by noting that for some parameter values the model (31){(32) can show periodic solutions which do not travel, like those shown in Sec. II. Likewise, the model in Sec. I can support travelling waves for = 2.

C. Winfree oscillators

One of the rst models of interacting oscillators studied is the Winfree model [2, 19, 29, 46]. We consider a spatially-extended network of Winfree oscillators whose dynamics are given by

$$\frac{d_j}{dt} = !_j + \frac{2Q(_j)}{N}\sum_{k=1}^{N} K_{jk}P(_k)$$

where $K_{jk} = K(2 jj kj=N)$ for some 2 -periodic $P(\ )$ K(2 coupling function K, $Q(\ ) = \sin =$ $p:$,

re

&

kdo wy28(v)28(es)]TJ0 513stabl5i4754(A8d4re)[(2)[W/52T

$z = -1$ is not a fixed point of Eq. (42), we can always choose $t_2 \in (0; 2\pi)$ such that $z(t) \neq -1$ for $t \in [t_1; 2\pi)$. Then the Mean Value Theorem implies

$$0 \leq |z(2\pi)|^2 - |z(t_1)|^2 = 2\frac{d|z|^2}{dt}(t_2) \qquad (44)$$

for some $t_2 \in (t_1; 2\pi)$. On the other hand, due to our assumptions, we have

$$\frac{d|z|^2}{dt} = 2\mathrm{Re}\left[\overline{c_0(t)}z(t) + c_1(t) + c_2(t)z(t)\right]$$

$$\leq 2c\,\mathrm{Re}(z(t) + 1)$$

and therefore

$$\frac{d|z|^2}{dt}(t_2) \leq 2c\,\mathrm{Re}(z(t_2) + 1) < 0.$$

This is a contradiction to (44), which completes the proof. ■

Remark 1 If the conditions of Proposition 2 are fulfilled, then the stable solution of Eq. (42) is also asymp-

ACKNOWLEDGEMENTS

The work of O.E.O. was supported by the Deutsche Forschungsgemeinschaft under Grant No. OM 99/2-2.

DECLARATIONS

Competing interests: The authors have no competing interests to declare that are relevant to the content of this article.

Code availability: Code for calculating any of the results presented here is available on reasonable request from the authors.

AUTHOR CONTRIBUTIONS

Conceptualization: C.R. Laing, O.E. Omel'chenko.
Formal analysis: C.R. Laing, O.E. Omel'chenko.
Funding acquisition: O.E. Omel'chenko.
Investigation: C.R. Laing, O.E. Omel'chenko.
Methodology: C.R. Laing, O.E. Omel'chenko.
Software: C.R. Laing.
Validation: C.R. Laing, O.E. Omel'chenko.
Visualization: C.R. Laing.
Writing { original draft: C.R. Laing, O.E. Omel'chenko.
Writing { review & editing: C.R. Laing, O.E. Omel'chenko.

of Brain and Behavior, chap. 37, pp. 505{517. Wiley-Blackwell, Hoboken, NJ (2017)
[29] Laing, C.R., Blasche, C., Means, S.: Dynamics of structured networks of Winfree oscillators. Front. Syst. Neurosci. 15, 631377 (2021)
[30] Laing, C.R., Longtin, A.: Dynamics of deterministic and stochastic paired excitatory-inhibitory delayed feedback. Neural Comput. 15(12), 2779{2822 (2003)
[31] Laing, C.R., Omel'chenko, O.: Moving bumps in theta neuron networks. Chaos 30(4), 043117 (2020)
[32] Laing, C.R., Troy, W.: PDE methods for nonlocal models. SIAM J. Appl. Dyn. Syst. 2(3), 487{516 (2003)
[33] Laing, C.R., Troy, W.C., Gutkin, B., Ermentrout, G.B.: Multiple bumps in a neuronal model of working memory. SIAM J. Appl. Math. 63(1), 62{97 (2002)
[34] Latham, P., Richmond, B., Nelson, P., Nirenberg, S.: Intrinsic dynamics in neuronal networks. I. Theory. J. Neurophysiol. 83(2), 808{827 (2000)
[35] Lee, W.S., Ott, E., Antonsen, T.M.: Large coupled oscillator systems with heterogeneous interaction delays. Phys. Rev. Lett. 103, 044101 (2009)
[36] Linden, H., Petersen, P.C., Vestergaard, M., Berg, R.W.: Movement is governed by rotational neural dynamics in spinal motor networks. Nature 610, 526{531 (2022)
[37] Montbrio, E., Pazo, D., Roxin, A.: Macroscopic description for networks of spiking neurons. Phys. Rev. X 5, 021028 (2015)
[38] Neto , T.I., Schi , S.J.: Decreased neuronal synchronization during experimental seizures. J. Neurosci. 22(16), 7297{7307 (2002)
[39] Omel'chenko, O.: Mathematical framework for breathing chimera states. J. Nonlinear Sci. 32(2), 1{34 (2022)
[40] Omel'chenko, O., Laing, C.R.: Collective states in a ring network of theta neurons. Proc. Royal Soc. A 478(2259), 20210817 (2022)
[41] Omel'chenko, O., Wolfrum, M., Laing, C.R.: Partially coherent twisted states in arrays of coupled phase oscillators. Chaos 24, 023102 (2014)
[42] Omel'chenko, O.E.: Nonstationary coherence-incoherence patterns in nonlocally coupled heterogeneous phase oscillators. Chaos30(4), 043103 (2020)
[43] Omel'chenko, O.E.: Periodic orbits in the Ott-Antonsen manifold. Nonlinearity 36, 845{861 (2023)
[44] Ott, E., Antonsen, T.M.: Low dimensional behavior of large systems of globally coupled oscillators. Chaos 18(3), 037113 (2008)
[45] Ott, E., Antonsen, T.M.: Long time evolution of phase oscillator systems. Chaos 19(2), 023117 (2009)
[46] Pazo, D., Montbrio, E.: Low-dimensional dynamics of populations of pulse-coupled oscillators. Phys. Rev. X 4, 011009 (2014)
[47] Pietras, B.: Pulse shape and voltage-dependent synchronization in spiking neuron networks. arXiv preprint arXiv:2304.09813 (2023)
[48] Pinto, D.J., Ermentrout, G.B.: Spatially structured activity in synaptically coupled neuronal networks: II. Lateral inhibition and standing pulses. SIAM J. Appl. Math. 62(1), 226{243 (2001)
[49] Ratas, I., Pyragas, K.: Macroscopic self-oscillations and aging transition in a network of synaptically coupled quadratic integrate-and- re neurons. Phys. Rev. E 94, 032215 (2016)
[50] Reyner-Parra, D., Huguet, G.: Phase-locking patterns underlying e ective communication in exact ring rate models of neural networks. PLOS Comput. Biol. 18(5), e1009342 (2022)
[51] Roxin, A., Brunel, N., Hansel, D.: Role of delays in shaping spatiotemporal dynamics of neuronal activity in large networks. Phys. Rev. Lett. 94(23), 238103 (2005)
[52] Schmidt, H., Avitabile, D.: Bumps and oscillons in networks of spiking neurons. Chaos 30, 033133 (2020)
[53] Schmidt, H., Avitabile, D., Montbrio, E., Roxin, A.: Network mechanisms underlying the role of oscillations in cognitive tasks. PLoS Comput. Biol. 14(9), e1006430 (2018)
[54] Segneri, M., Bi, H., Olmi, S., Torcini, A.: Theta-nested gamma oscillations in next generation neural mass models. Front. Comput. Neurosci. 14, 47 (2020)
[55] Shima, S., Kuramoto, Y.: Rotating spiral waves with phase-randomized core in nonlocally coupled oscillators. Phys. Rev. E 69(3), 036213 (2004)
[56] Strogatz, S.: From Kuramoto to Crawford: exploring the onset of synchronization in populations of coupled oscillators. Phys. D 143(1-4), 1{20 (2000)
[57] Uhlhaas, P.J., Singer, W.: Abnormal neural oscillations and synchrony in schizophrenia. Nature Rev. Neurosci. 11(2), 100{113 (2010)
[58] di Volo, M., Torcini, A.: Transition from asynchronous to oscillatory dynamics in balanced spiking networks with instantaneous synapses. Phys. Rev. Lett. 121, 128301 (2018)
[59] Wilczynski, P.: Planar nonautonomous polynomial equations: the riccati equation. J. Di er. Equ. 244, 1304{1328 (2008)
[60] Wimmer, K., Nykamp, D.Q., Constantinidis, C., Compte, A.: Bump attractor dynamics in prefrontal cortex explains behavioral precision in spatial working memory. Nature Neurosci. 17(3), 431{439 (2014)
[61] Zhang, K.: Representation of spatial orientation by the intrinsic dynamics of the head-direction cell ensemble: a theory. J. Neurosci. 16(6), 2112{2126 (1996)